Arch. Metall. Mater. **64** (2019), 1, 339-346

DOI: 10.24425/amm.2019.126257

P. GOLEWSKI*, T. SADOWSKI*#

# NUMERICAL AND LABORATORY TESTS OF ALUMINUM PROFILE CONNECTION USING THE "POPULAR LOCK"

Aluminum profiles play an important role in civil engineering (facades, walls with windows) as well as in mechanical engineering (production lines, constructions of 3D printers and plotters). To ensure quick assembly, disassembly or changed the dimensions of constructions it is not possible to use such methods as welding, adhesive or riveting joints. The solution may be to use the so-called "popular lock". It is a mechanism, the closure of which is caused by tightening of the conical screw, joining the "T" profile in the node. In order to properly design using the presented type of connection, it is necessary to know its strength and stiffness both in simple and complex loads states, also including imperfections. In the literature there is no information about the operation of the construction node with the so-called "popular lock".

The paper presents the results of experimental tests for connections subjected to uniaxial tensile test, paying special attention to the defects that may appear during the assembly. In the next step, a 3D solid connection model was created. Numerical simulations were performed in the Abaqus / Explicite program for both uniaxial tensile test and bending tests in two planes. Limit values of loads above which there is a plastic deformation of the material were determined. Determination of stiffness and strength of a single node allowed to make a simplified connector model. Using the numerical model, the analysis was performed taking into account the influence of imperfections on the work of the entire connection.

*Keywords:* bolt-channel, numerical simulation, popular lock, aluminium profile

## 1. Introduction

Aluminum constructions play an important role both in civil engineering (facades, supporting structures with large spread, roof coverings, window walls, handles, sliding gates) as well as in aviation (fuselage, wings). The following connections can be used to make aluminum constructions: adhesive [1-4,9,12], rivet [8-9,11], spot-welding [3-4], clinched [5-7], socked-pin (mechanical locking) [10,24,26], screws [22-23,25] and welded [13,17], however, they mainly concern connections of planar sheet. A very interesting method is the RSW (Resistance Spot Welding) and RFSSW (Refill Friction Stir Spot Welding), but it requires appropriate technological machines [18-21]. For joining aluminum profiles, most of these methods have limited application, in particular when the connection must be disjoint. Everywhere, where fast assembly or changing the shape of the structure is needed, connections with use of so-called locks become irreplaceable. The "popular lock" is a mechanism based on a T-slot connection widely used in numerical machine tables, plotters or measuring tables for fixing workpieces or measuring tools. The general definition of a connection using a groove in one of the profiles and a properly shaped bolt or nut is called "Bolt Chanel".

In work [14], both experimental and numerical tests were used for the mechanical connection of an aluminum profile with a steel intermediate element. This is a convenient solution because aluminum profiles often have channels and thus a construction node can be made anywhere without affecting the structure of the profile. In this case, the intermediate element was a steel nut to which the further part of the structure or the applied load could be attached. For this type of connection, several tests must be carried out: shear, bending and tensile test (pulling off the nut). The results of such tests are valuable information for designers using the aluminum profiles. A numerical model was also presented and subjected to analysis in the Abaqus program. The finite element method is an approximate method, therefore the authors take particular care in:

- calculation for three mesh densities in the range from 5 mm to 1mm of the global dimension of the finite element,
- taking into account the influence of imperfection in the range from the perfect model to 0.5 mm of clearance.

In the given range of mesh densities, the same results were obtained. However, the size of imperfection has a significant impact on the force-displacement curve, but for the load after crossing the yield point. For the elastic range, the influence of imperfection is negligible. The authors also compared the results

---

* LUBLIN UNIVERSITY OF TECHNOLOGY, FACULTY OF CIVIL ENGINEERING AND ARCHITECTURE, DEPARTMENT OF SOLID MECHANICS, 40 NADBYSTRZYCKA STR., 20-618 LUBLIN, POLAND

# Corresponding author: t.sadowski@pollub.pl

of the FEM simulation with a laboratory test, obtaining a good convergence of results.

In [15] the authors analyzed the connection of a column with a beam using a "T" type connector. The "T" type connector is characterized by a large number of parameters, which impact was analyzed by the authors. Among these parameters we can distinguish: dimensions of front plate, distance of fasteners from the edges of front plate, pitch, diameter of fasteners and material from which they were made. It should be noted that in the numerical model the connectors were made in a simplified way using cylinders with different diameters (mandrel and head). The tests were carried out with one load scheme.

In [16] the authors analyzed the π type bolt connection in which the socket was made of aluminum and fiber composites. The tests were carried out during bending and allowed to determine the load capacity of the joint. For an aluminum socket about 21% less force causing damage was achieved. However, the amount of work on the implementation of this type of connection is much smaller for the aluminum model than composite, because it can be made on numerical machines or using extrusion. The numerical model was made in the Abaqus program and good convergence of results with a laboratory test was obtained.

In summary, the issue regarding the calculation of connections of aluminum structures is still valid. In this area, not only experimental studies are carried out, but also FEM simulations. However, in the literature, no information was found on connection studies using so-called "popular lock" with dimensions 16×16. Therefore, the present paper will fill this gap, including complete analysis of both: experimental and numerical results.

## 2. Construction of a connection using the "popular lock"

In order to properly design with using presented type of connection, the knowledge about its strength and stiffness is needed in both simple and complex load states, also taking into account imperfections. The popular lock 16×16 cooperating with A-4858 aluminum profile, was chosen for the research. The "lock" presented in the exploded view in Fig. 1b, consists of 5 parts. The body (1) is made of plastic and does not carry loads. An important element is the spindle (2) which on the one end has a "T" shape (fixed in the profile), and on the other end has a conical seat, by which the load is transferred to the sleeve (3) and next by the holdfast (4) to the hole in the profile. The spring (5) is designed for ease of assembly by pushing the spindle. Closing of the connection takes place by tightening the holdfast (4) which causes compression of the connection.

When using the "popular lock", it is necessary to maintain an appropriate tolerance when cutting profiles and drilling the hole used for mounting the lock sleeve. Connection is made properly, if the sleeve is fitted in a hole made in the profile, as shown in Fig. 2b. If the sleeve is only partially in contact with the hole, the connection must be considered as faulty. Differences between the results obtained for both the correct and faulty connection will be shown in the next paragraph.

The analyzed node consisted of two sections of aluminum profile with the number A-4858 39.5/19.5/9 and 16×16 "popular lock". The lengths of the profile sections were 8 cm and 10 cm. The dimensions of the profile section and the tested nodes are shown in Fig. 3.

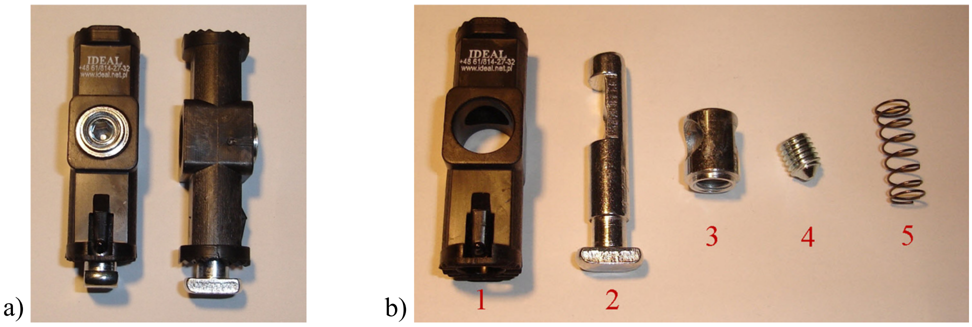

Fig. 1. a) popular lock, b) parts of the lock (1 – body, 2 – spindle, 3 – sleeve, 4 – holdfast, 5 – spring)

a) Faulty connection b) Correct connection c) Faulty connection

Fig. 2. Different types of connections

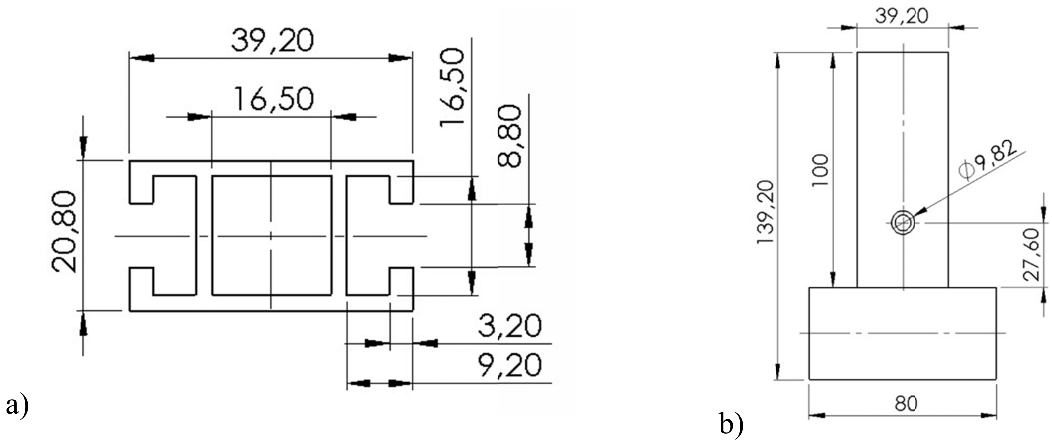

Fig. 3. Dimensions of: a) aluminium profile, b) tested node

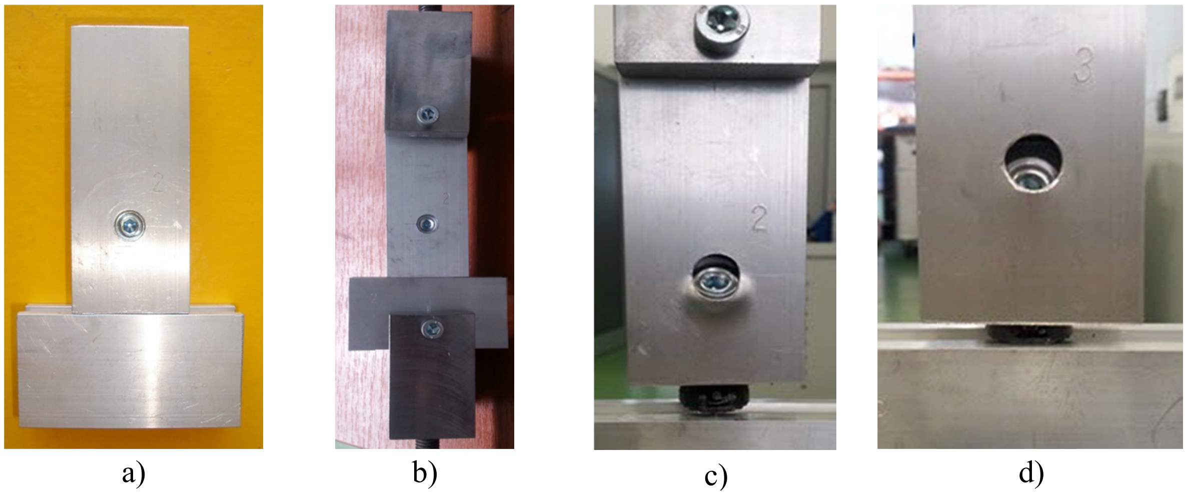

Fig. 4. Tested connection: a) after assembly, b) after mounting adapters, c) node No. 2 during test, d) node No. 3 during test

### 3. Laboratory tests

Experimental tests were carried out for the uniaxial tensile for three samples, one of which is visible in Fig. 4a. In order to mount the nodes in the grips of the testing machine, each of the samples (nodes) was properly prepared for testing by drilling a hole, allowing for mounting of additional adapters (Fig. 4b). Static tensile test was carried out on the 100kN MTS testing machine.

For node No. 2, it can be observed that in the first tensile phase, the walls of the hole made in the profile and the socket of the sleeve interact with each other, which causes its rotation and the formation of significant plastic deformations around the hole (Fig. 4c). In the subsequent phases of the study, cracks in the sample material around the hole and further rotation of the connector are visible.

In the case of testing node No. 3, from the beginning one can observe an asymmetric change of the holdfast position in relation to the sleeve. In Fig. 4d there is no visible plastic deformation around the hole. In the subsequent phases, the lock from the profile gradually comes out. In the case of nodes 1 and 3, there is no cracking in the material of the aluminum profile, so the energy to disconnect the node was much smaller compared to the correctly made node No. 2.

Figure 5 shows the graphs for the three examined nodes. Nodes No. 1 and No. 3 behave similarly and the maximum force value is at the level of 2 kN, however, it occurs for large displacements 8-10 mm, in the range in which the node operation is unacceptable. Correctly made node No. 2 is characterized by not only greater strength (maximum strength is at 4 kN), but also greater stiffness.

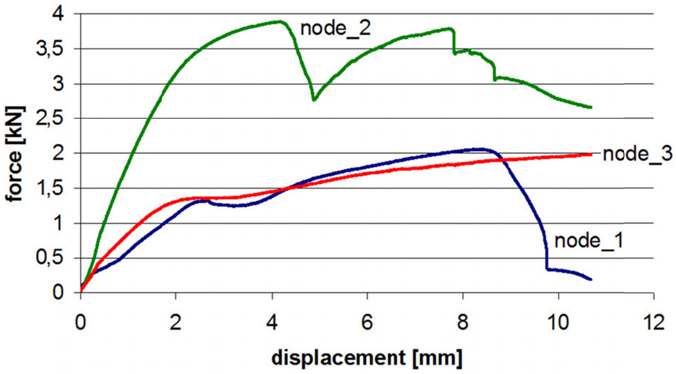

Fig. 5. Force – displacement graph

## 4. Numerical studies

During assembly of the connections, it was found that there are clearances between the lock parts and between the lock and the profile. Some of them make it easier to assemble the lock in the profile, however, such inaccuracies must have a negative effect on the connection, resulting in an asymmetrical load on the profile walls.

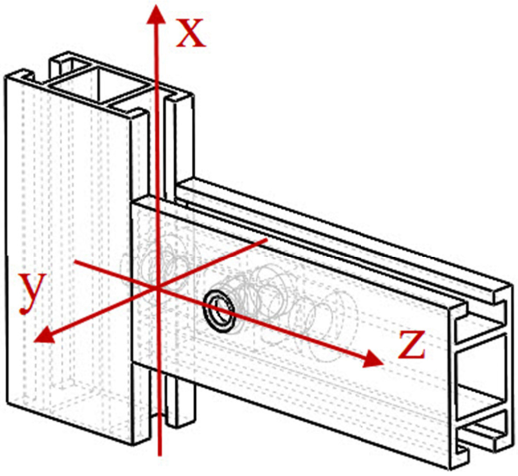

Fig. 6. Node model

Numerical tests were carried out for the 4 models taking into account three types of loads:

1. Tensile along the Z-axis – exact model (model 1).
2. Y-axis bending (model 2).
3. X-axis bending (model 3).
4. Tensile along the Z axis – model with imperfections (model 4).

### 4.1. Preparation of the CAD model

Numerical tests were preceded by geometry measurements of all parts of the lock (Fig. 7) as well as mappings in the CAD program. During making models, it was noticed that in several places there was clearance eg between the spindle (2) and the body (1) or the hole in the sleeve (3) and the spindle (2). These clearances were not included in the first three models and all surfaces were in contact with each other. In CAD modeling, no spring was considered, which only serves as an auxiliary role during assembly, pushing the spindle (2) while loosening the holdfast (4) (releasing the lock). During the modeling, a simplification was made in the part (3) and (4) by resigning of the thread.

### 4.2. Preparation of the FEM model

In order to avoid problems with the generation of the FEM mesh, it was necessary to partition individual parts of the assembly. The total number of finite elements divided into individual parts of the assembly is shown in Table 1. It should be noted that for parts 1 and 5, both cubic and tetrahedral elements were used, which adapt better to complicated shapes.

TABLE 1

Quantities of finite elements

| | **C3D8R** | **C3D4** | **C3D6** |
|---|---|---|---|
| 1. Spindel | 8228 | 12638 | 350 |
| 2. Sleeve | 216 | 17750 | — |
| 3. Holdfast | 1276 | — | 66 |
| 4. Body | 7132 | 25997 | 280 |
| 5. Profile 8 cm | 14720 | — | — |
| 6. Profile 10 cm | 16744 | — | — |

In Table 1, finite element designations mean:

– the C3D8R element is a 8-node general purpose linear brick element, with reduced integration (1 integration point),

– the C3D6 element is a 6-node general purpose wedge element (2 integration points),

– the C3D4 is a 4-node general purpose tetrahedral element (1 integration point).

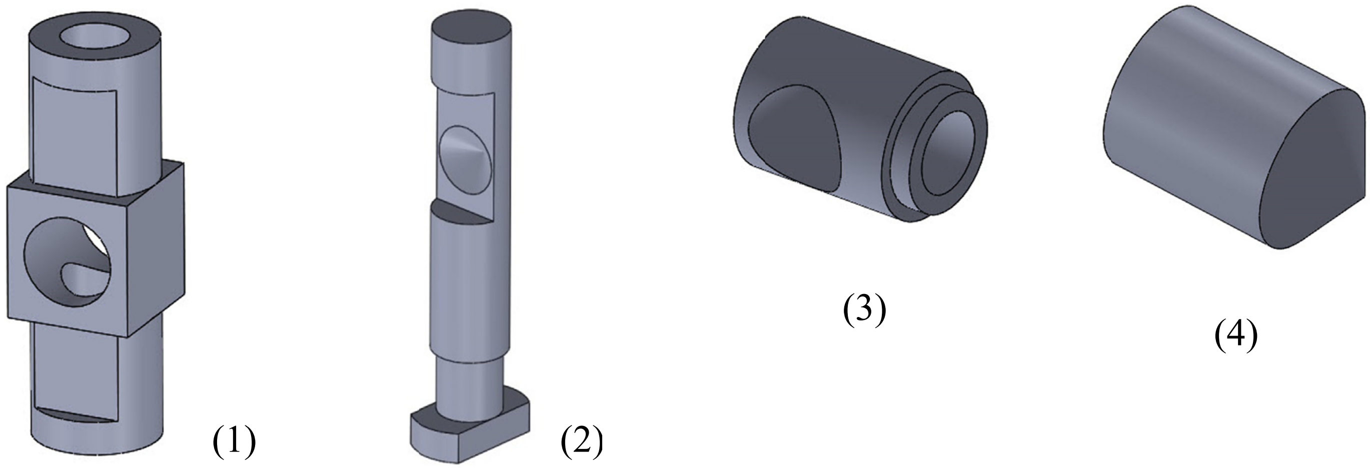
(1) (2) (3) (4)

Fig. 7. CAD model of „popular lock" parts: (1) body, (2) spindle, (3) sleeve, (4) holdfast

At the boundary of these two different meshes, ties constraints were created. The tie constraints were also used between the cylindrical surface of parts 2 and 3. In the real model there is a thread there, which was not included in the modeling due to the high degree of complexity of the geometry.

The material from which the profiles were made is a 6060 alloy. In the numerical calculations for both aluminum profiles and steel parts of the lock, the elastic – plastic material model was used with properties as in Table 2.

TABLE 2

Material properties for 6060 alloy used in simulations

| | ***E*, [GPa]** | ***ν*, [-]** | **$R_H$, [MPa]** | **$R_m$, [MPa]** | ***A*, [%]** |
|---|---|---|---|---|---|
| aluminum | 69.5 | 0.33 | 150 | 190 | 6 |
| steel | 200 | 0,3 | 235 | 410 | 21 |

where: $E$ – Young's modulus, $\nu$ – Poisson's ratio, $R_H$ – yield strength, $R_m$ – tensile strength, $A$ – elongation at break

The polymer part (1) was treated as perfectly elastic with the Young's modulus $E = 2355$ MPa. It is not an element involved in the load transfer, it only fulfills the role that determines the position of the spindle and sleeve.

The next step was to define boundary conditions, according to Fig. 8. For surfaces 1 and 2, all degrees of freedom were encastre. Surface 3 was connected to the reference point RP-1 by using coupling constraints. The goal was to apply loads more easily. There were many contact pairs in the model that were not selected in a "manual" way. In this case, general contact was used. The friction coefficient with value of 0.1 was assumed. The prepared models were calculated in the Abaqus / Explicite program.

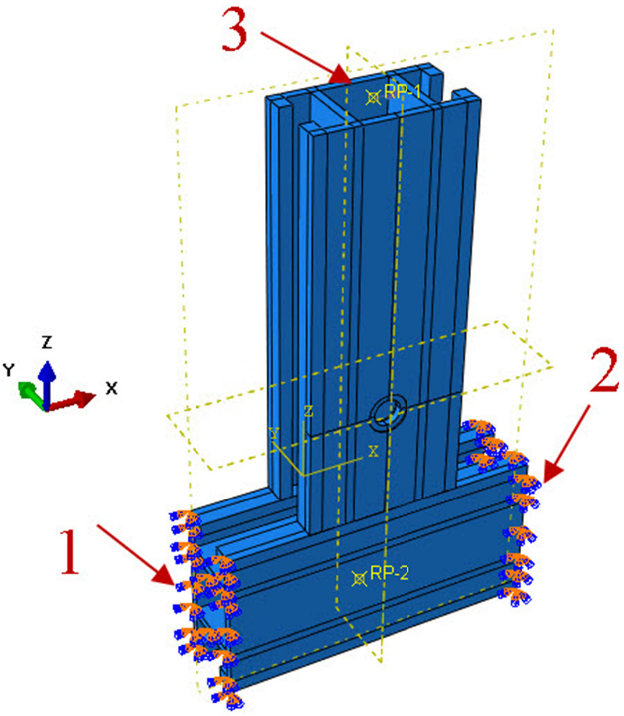

Fig. 8. Boundary conditions

### 4.3. The results of FEM simulation

The uniaxial tensile simulation (model 1) was performed by causing the displacement along the Z axis for the RP-1 reference point. The final effect of the simulation was to bend the channel walls of the aluminum profile to such an extent, that the node was disconnected. Despite a local plastic deformations of the aluminum profile, at the point of contact of the hole with the sleeve, it was not displaced or rotated as it was in the laboratory test. As a result of the FEM simulation it was found that the limit state was reached for a displacement of 0.2 mm which corresponded to the tensile force of 2009 N. For this load value, plastic deformation occured at the contact point of the sleeve with the hole. The distribution of the Huber – von Mises – Hencky (H-M-H) reduced stresses in all assembly parts is shown in Fig. 9.

According to the FEM simulation for the bending moment relative to the y axis (model 2), the safe condition was achieved for the value of 28.75 Nm, which corresponded to the angle of rotation of 0.45°. For the bending moment relative to the x-axis (model 3), the safe condition was achieved at the value of 25.5 Nm, which corresponded to the rotation angle of 0.019°. The distributions of the H-M-H reduced stresses in all assembly parts are shown in Figure 10.

## 5. Analysis of test results

The results of the FEM simulation and the results of the laboratory test for node No. 2 are shown in the graph (Fig. 11). Comparing the results for the 4mm of displacement, forces of 5.52 kN and 3.87 kN were obtained for the FEM result and laboratory test, respectively. However, such a large difference, should not be treated as an error during the simulation. It should be emphasized that the geometric CAD model was perfect and did not have any clearances.

After making accurate measurements of the lock body (1), the following results were obtained: 16.27 mm and 16.18 mm, while the dimensions of the socket in the aluminum profile were 16.5 mm × 16 mm × 5 mm. Similar values of clearance were also present between the steel spindle and the sleeve and body. Therefore, an additional simulation was performed for a model closer to the real one (model 4), the results of which are shown in Fig. 12.

The results of the numerical model demonstrate that the presence of imperfections in the form of clearance is very important and their inclusion allowed to get close to the real result. However, it is difficult to take into account all inaccuracies as their mapping would require geometry scanning and its subsequent processing. Thus, the further work should focus on improving of the geometry of the lock and an increase in load capacity of the node through changes in its construction.

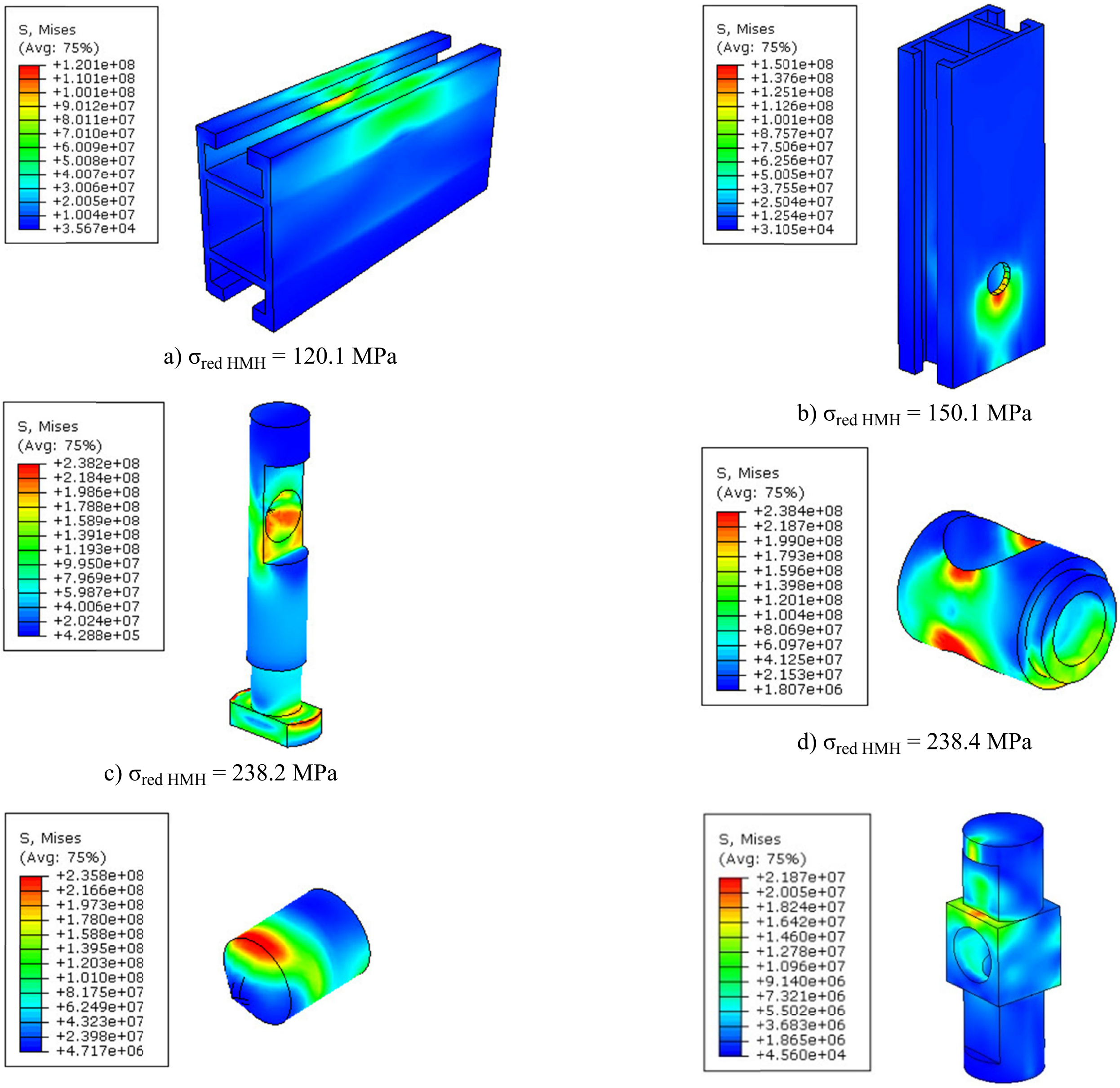

a) $\sigma_{\mathrm{red\ HMH}} = 120.1$ MPa

b) $\sigma_{\mathrm{red\ HMH}} = 150.1$ MPa

c) $\sigma_{\mathrm{red\ HMH}} = 238.2$ MPa

d) $\sigma_{\mathrm{red\ HMH}} = 238.4$ MPa

c) $\sigma_{\mathrm{red\ HMH}} = 235.8$ MPa

c) $\sigma_{\mathrm{red\ HMH}} = 21.8$ MPa

Fig. 9. Mises stresses for tensile load with value of 2009 N

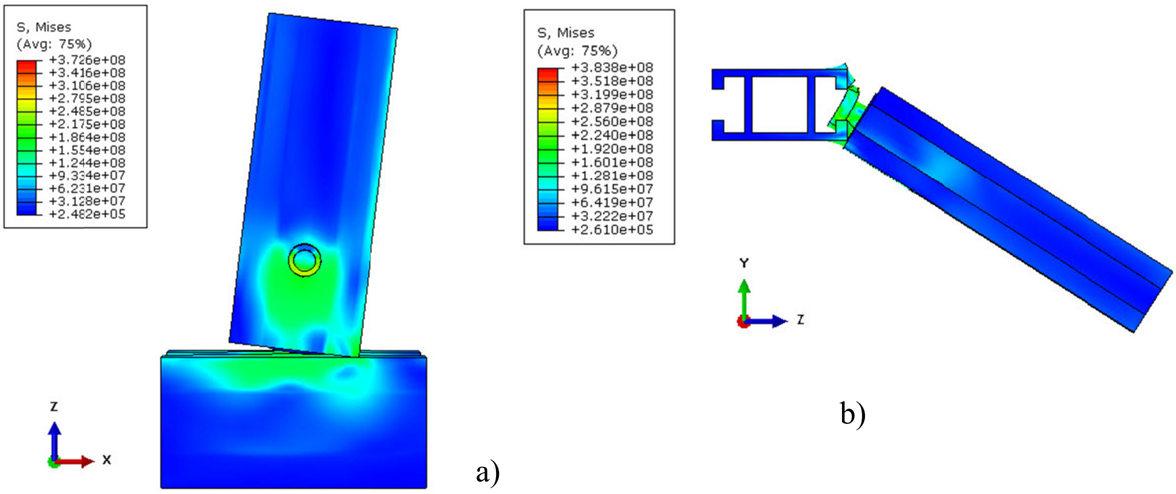

a)

b)

Fig. 10. Results for bending a) relative to the y axis b) relative to the x axis

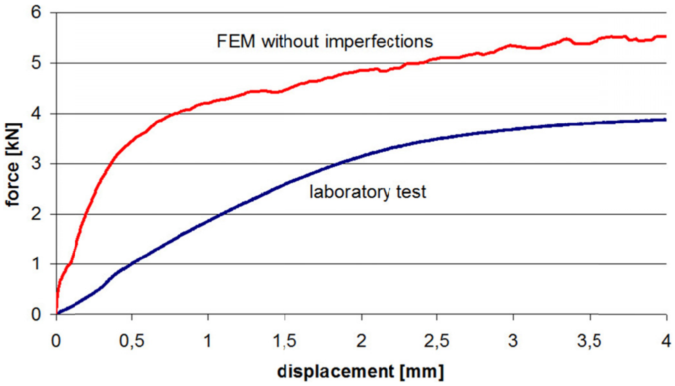

Fig. 11. Comparison of results for tensile tests

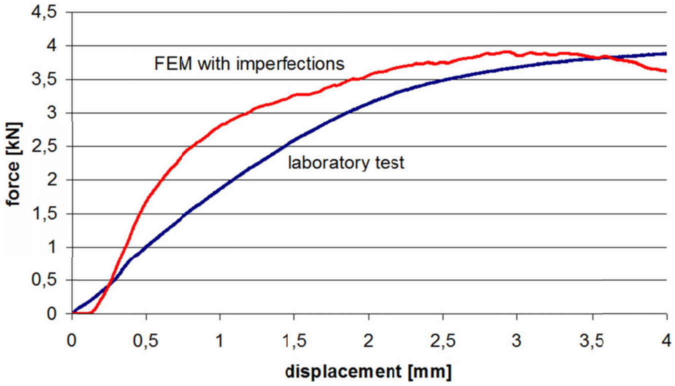

Fig. 12. The influence of imperfections in numerical model

## 6. Conclusions

The paper presents the method of determining the load capacity of a node made of aluminum profiles using both laboratory tests and numerical calculations. The following conclusions flow from the presented work.

1. Implementation of the connections using the popular lock is a beneficial method due to the high speed of node entering to the construction and the lack of the need to use specialized tools such as TIG welder.
2. During making the joint, the perpendicularity of the profile cutting plane must be maintained. Careless cut, results in assembly errors as shown in Figure 2 and a half smaller force disconnecting the node.
3. As a result of laboratory tests, the tensile load capacity of the node at the level of 3.87 kN was obtained, and numerical tests gave the value of 5.52 kN. However, it should be noted, that in this case the numerical model was ideal (did not have any imperfections).
4. Based on the numerical model, the limit values of loads above which the material is plasticized were determined. These are important values when performing calculations using connectors.
5. In the real model there are clearances with values in the range of 0.23 mm - 0.32 mm. Their inclusion allowed to approach the value obtained in the laboratory test.

The presented topic will be developed to include damage mechanisms during multiple closing and opening cycles of the joint. Different damage concepts presented e.g. in [27-37] can be used to extend theory of the snap-fit joints having the thermo-bimaterial effect.

### Acknowledgement

This work was financially supported by Ministry of Science and Higher Education (Poland) within the statutory research number S/20/2018.
The authors are grateful to dr M.Kneć for help in samples testing.

## REFERENCES

[1] L.F.M. da Silva, P.J.C. das Neves, R.D. Adams, J.K. Spelt, Int. J. Adhes. & Adhes **29**, 319-330, (2009).

[2] L.F.M. da Silva, P.J.C. das Neves, R.D. Adams, J.K. Spelt, Int. J. Adhes. & Adhes **29**, 331-341 (2009).

[3] T. Sadowski, P. Golewski, M. Kneć, Comp. Struct. **112**, 66-77 (2014).

[4] T. Sadowski, M. Kneć, P. Golewski, J. of Adhesion **90**, 346-364 (2014).

[5] T. Sadowski, T. Balawender, Technology of Clinch – Adhesive Joints, in Hybrid adhesive joints. Advanced Structured Materials **6**, Springer 2011, L.F.M. da Silva, A. Pirondi, A. Öschner (Eds), pp. 149-176.

[6] T. Balawender, T. Sadowski, J. Adhes. Sci. Technol. **25**, 2391-2407 (2011).

[7] T. Balawender, T. Sadowski, P. Golewski, Comput. Mater. Sci. **64**, 270-272 (2012).

[8] T. Sadowski, P. Golewski, Arch. Metall. Mat. **58**, 581-587 (2013).

[9] P. Golewski, T. Sadowski, Int. J. Adhesion and Adhesives **77**, 174-182 (2017).

[10] T. Sadowski, P. Golewski, V. Radoiu, Solid State Phenomena **254**, 1-7 (2016).

[11] T. Sadowski, P. Golewski, Key Eng. Mater. **607**, 49-54 (2014).

[12] T. Sadowski, M. Nowicki, D. Pietras, P. Golewski, Int. J. Adhesion and Adhesives **89**, 72-81 (2019).

[13] D. Loveborn, J.K. Larsson, K.A. Persson, Physics Procedia **89**, 89-99 (2017).

[14] L. Fiorino, V. Macillo, F.M. Mazzolani, Construc. Build. Mater. **73**, 76-88 (2014).

[15] G. De Matteis, M.T. Naqash, G. Brando, Eng. Struct. **41**, 548-561 (2012).

[16] L. Zhou, D. Zhang, L. Zhao, X. Zhou, J. Zhang, F. Liu, Mater. Design **98**, 201-208 (2016).

[17] P. Lacki, K. Adamus, Comp. and Struct. **89**, 977-985 (2011).

[18] P. Lacki, A. Derlatka, Comp. Struct. **159**, 491-497 (2017).

[19] P. Lacki, J. Niemiro, Comp. Struct. **159**, 538-547 (2017).

[20] K. Adamus, J. Adamus, J. Lacki, Comp. Struct. **202**, 95-101 (2018).

[21] P. Lacki, A. Derlatka, Comp. Struct. **202**, 201-209 (2018).

[22] P. Lacki, J. Nawrot, A. Derlatka, J. Winowiecka, Comp. Struct. **211**, 244-253 (2019).

[23] Ch.-Ko. Chao, Ch.-Ch. Hsu, J.-L. ang, J. Lin, Clin. Biom. **22**, 59-66 (2007).

[24] L.M. Alves, C.M.A. Silva, P.A.F. Martins, J. of Mat. Proc. Techn. **242**, 196-204 (2017).

[25] N. Sase, K. Nishioka, S. Koga, H. Furii, J. of Mat. Proc. Techn. **77**, 209-215 (1998).

[26] T. Markovits, A. Bauernhuber, M. Géczy, Phys. Proc. **39**, 100-107 (2012).

[27] H. Dębski, T. Sadowski, Comput. Mater. Sci. **83**, 403-411 (2014).

[28] G. Golewski, T. Sadowski, Constr. Build. Mater. **51**, 207-214 (2014).

[29] L. Marsavina, E. Linul, D.M. Constantinescu, D. Apostol, T. Voiconi, T. Sadowski, Eng. Fract. Mech. **129**, 54-66 (2014).

[30] M. Birsan, T. Sadowski, L. Marsavina, D. Pietras, Int. J. Solids Struct. **50**, 519-530 (2013).

[31] T. Sadowski, J. Bęc, Comput. Mater. Sci. **50**, 1269-1275 (2011).

[32] J. Gajewski, T. Sadowski, Comput. Mater. Sci. **82**, 114-117 (2014).

[33] T. Sadowski, A. Neubrand, Int. J. Fract. **127**, L135-L140 (2004).

[34] T. Sadowski, L. Marsavina, Comput. Mater. Sci. **50**, 1336-1346 (2011).

[35] T. Sadowski, Comput. Mater. Sci. **64**, 209-211 (2012).

[36] V. Burlayenko, H. Altenbach, T. Sadowski, S.D. Dimitrova, Comput. Mater. Sci. **116**, 11-21 (2016).

[37] T. Sadowski, L. Marsavina, N. Peride, E.M. Craciun, Comput. Mat. Sci. **46**, 687-693 (2009).